Evaluation of Virtual Inertia Control Strategies for MMC-based HVDC Terminals by P-HiL Experiments

[*]Salvatore D'Arco [*]Tuan T. Nguyen [*,†]Jon Are Suul

[*]SINTEF Energy Research
7465 Trondheim, Norway
salvatore.darco@sintef.no
thanhtuan.nguyen@sintef.no

[†]Department of Engineering Cybernetics
Norwegian University of Science and Technology
7495 Trondheim, Norway
jon.are.suul@ntnu.no, Jon.A.Suul@sintef.no

***Abstract*— This paper presents an experimental performance evaluation of different control strategies for providing virtual inertia from power electronic converters. The evaluation is based on a laboratory-scale prototype of a point-to-point HVDC transmission system with Modular Multilevel Converters (MMCs). Operation with a grid emulator connected to a real-time simulator reproduces the behavior of a power system and allows Power-Hardware-in-the-Loop (P-HiL) experiments. Control of the inverter terminal for providing virtual inertia to the simulated power system is evaluated with four different control system implementations. The four cases include a conventional control system enhanced with df/dt-based inertia emulation functionality and three different Virtual Synchronous Machine (VSM) implementations based on emulation of a synchronous machine swing equation. The dynamic response in the power flow and the frequency transients are evaluated for all cases, and the inertial energy exchanged with the isolated power system is assessed in comparison to a conventional power controller without inertia emulation. The results demonstrate that all the evaluated implementations can provide similar inertial response when operated in a small isolated grid, while clear differences in dynamic response and stability properties are revealed during operation under strong grid conditions.**

Keywords—HVDC Transmission, Modular Multilevel Converters, Virtual Inertia, Virtual Synchronous Machines

I. INTRODUCTION

The increasing utilization of renewable energy sources with power electronic grid interfaces and the correspondingly declining capacity of large synchronous generators operating in the power system is leading to concerns on the reduced equivalent system inertia [1]-[4]. Thus, control methods for providing virtual inertia from power electronic converters have been widely proposed during the last decade [5]-[10]. These control methods are commonly referred to as inertia emulation (IE), Virtual Synchronous Generators (VSGs) or Virtual Synchronous Machines (VSMs) since one of the main control objectives is to emulate the inertial behaviour of a synchronous generator (SG). While many of the first proposals for control methods with IE of VSG/VSM functionality were intended for distributed generation sources like wind turbines and energy storage systems, implementations adapted for a wide range of applications have been studied during the last decade.

The converter terminals of Voltage Source Converter (VSC) -based HVDC transmission schemes can be of particular interest for providing virtual inertia in large-scale power grids due to their high power rating and the potentially significant impact on the local grid operation. Thus, several studies of HVDC converter operation for providing virtual inertia, and corresponding proposals for control strategies, have been presented in recent publications [11]-[18]. While new VSC HVDC systems are usually based on Modular Multilevel Converter (MMC) technology, most previous studies of control strategies for providing virtual inertia have assumed simplified converter models corresponding to 2-level VSCs. Although some recent publications have considered implementation of virtual inertia control (VIC) for MMC-based HVDC systems, as for instance [19]-[21], the detailed interaction with the inertial response of a power system has not been studied in detail. Furthermore, experimental demonstrations of MMCs controlled for providing virtual inertia under realistic network conditions are not available in the literature.

In this paper, a Power-Hardware-in-the-Loop (P-HiL) laboratory setup is utilized to provide an experimental assessment of control methods for providing virtual inertia from an HVDC terminal. The P-HiL configuration allows for combining the physical hardware of a laboratory scale MMC-based HVDC interconnection with the real-time simulation of a power system. The dynamic responses obtained with four different control system implementations for providing virtual inertia are presented in comparison to the response of a conventional control strategy. The P-HiL experiments are conducted for an isolated power system configuration with low equivalent inertia as well as for operation in a strong grid. Furthermore, the obtained results are utilized to evaluate the transient energy exchange between the converter providing virtual inertia and the simulated grid. The results demonstrate how all the investigated schemes can provide the desired inertial response when interfaced with a low inertia network, although with minor differences in the dynamic response and the exchanged energy. For operation under strong grid conditions, the differences in dynamic response for the various control systems are more noticeable, and clear differences in damping of inertial oscillations can be observed. This indicates that control methods for providing virtual inertia should be

This work was supported by the project "HVDC Inertia Provision" (HVDC Pro), financed by the ENERGIX program of the Research Council of Norway (RCN) with project number 268053/E2, and the industry partners; Statnett, Statoil, RTE and ELIA.

This is the accepted version of an article published in Proceeding 45th Annual Conference of the IEEE Industrial Electronics Society - IECON 2019
http://dx.doi.org/10.1109/IECON.2019.8927704

carefully assessed under the full range of expected operating conditions, but that operation connected to a strong grid can be considered a worst-case condition suitable for initial evaluation of small-signal stability.

II. Converter Control for Providing Virtual Inertia

The control of power electronic converters to provide virtual inertia implies the need to emulate the inertial behaviour of a grid-connected synchronous machine (SM). Since the inertial response can be emulated without replicating all the electrical dynamics of an SM, it is usually preferred to base control strategies for inertia emulation on the simplified swing equation of an SM [8].

A. Swing equation of a Synchronous Machine

The inertial dynamics of a synchronous machine is determined by the torque balance of the rotor given as

$$J\frac{d\Omega}{dt} = \tau_m - \tau_{el} \tag{1}$$

Where J is the inertia, Ω is the mechanical speed, τ_m is the mechanical torque on the shaft and τ_{el} is the electrical torque of the machine. For power system studies, the inertial dynamics are more commonly expressed by a power balance [22]. Assuming small deviations around the nominal grid frequency and representing the dynamics in per unit quantities, the traditional swing equation of an SM can then be expressed as:

$$\frac{d\omega}{dt} = \frac{p_m}{T_a} - \frac{p_o}{T_a} - \frac{p_d}{T_a} \tag{2}$$

where ω is the per unit speed, p_m is the mechanical input power, p_o is the electrical output power and p_d is the damping power generated by the SM damper windings during transients in the rotor speed. The inertia of the SM is in this equation expressed by the mechanical time constant $T_a = 2H$, where H is the inertia constant of the machine.

B. Frequency-derivative-based Inertia Emulation

A simple way to emulate the transient power flow resulting from the inertial dynamics of (2) is to consider the power flow that would result from the acceleration of T_a in response to variations in the grid frequency ω_g. Ignoring the damping term in (2), the power flow associated with the SM swing equation would be proportional to the inertia time constant and the derivative of the grid frequency. Thus, a simple control strategy for inertia emulation (IE) can be expressed as [23]

$$\Delta p^*_{IE} = -T_a\frac{d\omega_g}{dt} \tag{3}$$

Such frequency-derivative-based Inertia Emulation (*df/dt* IE) can be implemented in power electronic converters by introducing Δp^*_{IE} from (3) as an incremental power reference in the control system. However, the derivative of the grid frequency is not available in the control system of a power electronic converter and will usually be estimated from voltage measurements by a Phase Locked Loop (PLL). To avoid amplification of noise due to the derivative term in (3), a limited derivative or a low-pass filtering of the frequency derivative is usually added in the implementations of *df/dt* IE [24], [23]. Introducing also primary frequency control to emulate the steady-state power-frequency droop characteristics

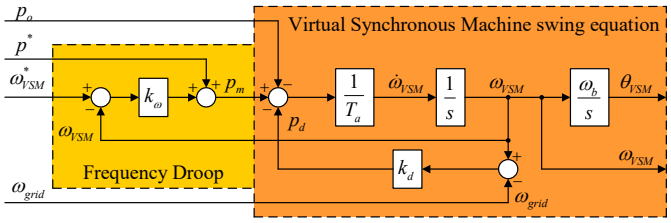

Fig. 1. Virtual Swing equation with frequency droop control

typically applied in SM governors, the power reference for *df/dt* IE control of a power electronic converter can be expressed as:

$$\Delta p^*_{IE} = -T_a\frac{s\omega_{LPf}}{s+\omega_{LPf}}\omega_{PLL} + k_\omega\left(\omega^* - \omega_{PLL}\right) \tag{4}$$

where ω_{PLL} is the grid frequency estimated by the PLL, k_ω is the power-frequency droop gain, ω^* is the reference frequency for the droop and ω_{LPf} is the crossover frequency of a low-pass filter applied to the estimated grid frequency derivative.

C. Virtual Synchronous Machine-based Control

Another general way to emulate the inertial dynamics of a SM is to directly emulate the SM swing equation according to (2). When including also a power-frequency droop, the dynamic equation to be emulated for such a Virtual Synchronous Machine (VSM) can be expressed as [26]:

$$\frac{d\omega_{VSM}}{dt} = \frac{p^*}{T_a} - \frac{p_o}{T_a} - \frac{k_d\left(\omega_{VSM} - \omega_{PLL}\right)}{T_a} - \frac{k_\omega\left(\omega_{VSM} - \omega^*\right)}{T_a} \tag{5}$$

where ω_{VSM} is the speed of the emulated inertia. In this equation, the damping power p_d is expressed by a damping coefficient k_d and the difference between the virtual rotor frequency and the grid frequency, as commonly approximated for an SM swing equation. The implementation of the damping term can be based on a PLL as indicated in (5), or on any other method for estimating the grid frequency.

For controlling a power electronic converter as a VSM, the simulated swing equation according to (5) should be used for grid synchronization, which will ensure that the converter operates with a similar power-balance-based grid synchronization mechanism as a SM. A block diagram showing the implementation of the virtual swing equation from (5) for a VSM is shown in Fig. 1. This figure also indicates how the phase angle θ_{VSM} to be used for grid synchronization is resulting directly from the integral of the simulated rotor speed.

III. Evaluated Methods for Virtual Inertia Control of MMC-based HVDC Interconnections

The core of the VIC implementations investigated in this paper is the emulation of an SM swing equation according to either (4) or (5). However, additional control loops are required for operating an MMCs for providing virtual inertia. In the following, three different implementations of VSM-based control strategies and one implementation of *df/dt* IE are presented as basis for the experimental evaluation.

A. Current Controlled VSM

Two different implementations of a Current Controlled Virtual Synchronous Machine (CCVSM) are considered, based on [25]. An overview of the general control structure of a VSM is displayed in Fig. 2 a), with the structure of the inner loop

This is the accepted version of an article published in Proceeding 45th Annual Conference of the IEEE Industrial Electronics Society - IECON 2019
http://dx.doi.org/10.1109/IECON.2019.8927704

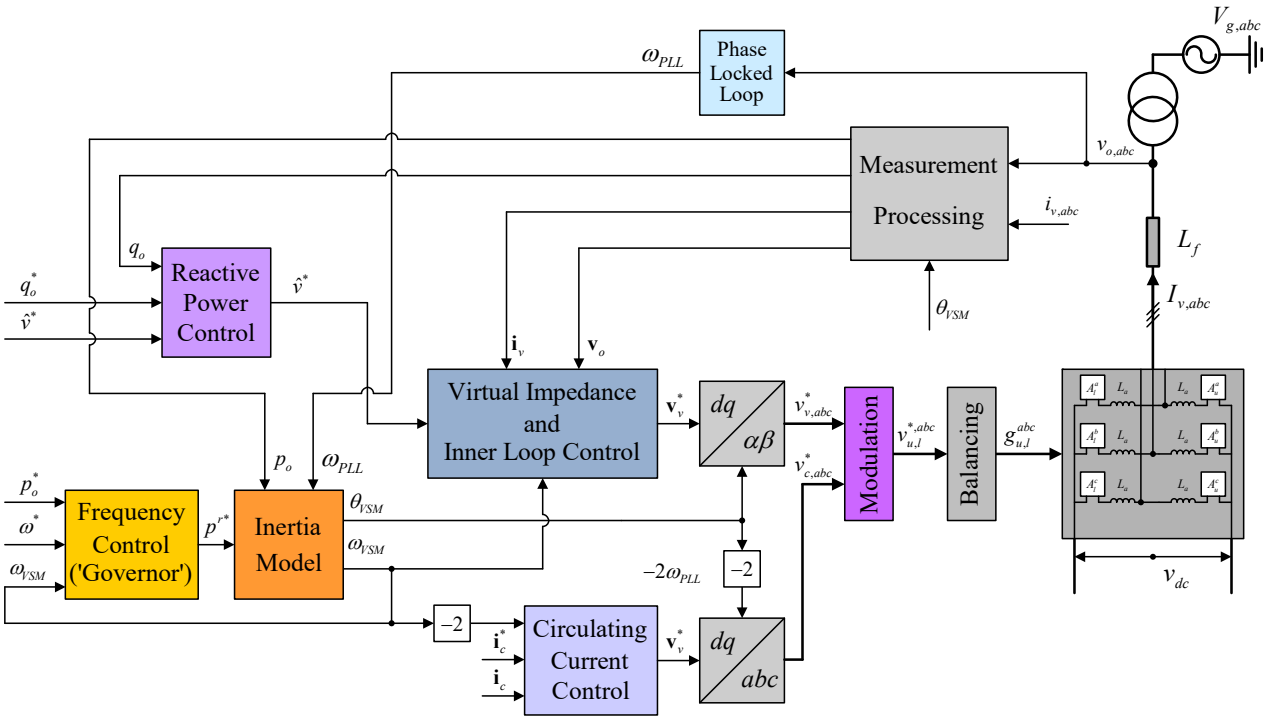

a) General overview of control structure for Virtual Synchronous Machines

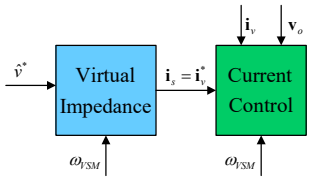

b) Configuration of virtual impedance and inner loop current controller for Current Controlled VSM (CCVSM)

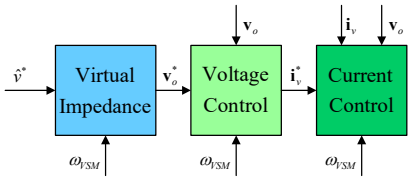

c) Configuration of virtual impedance and inner cascaded voltage and current controllers for Voltage Controlled VSM (VCVSM)

Fig. 2. Control schemes for CCVSM and VCVSM

control detailed in Fig. 2. As shown by Fig. 2 a), a reactive power controller generates a voltage amplitude setpoint. This voltage amplitude reference is utilized together with a virtual impedance to produce the current references for control of the ac-side currents of the converter, as shown in Fig. 2 b). The virtual impedance can represent the equivalent series impedance of an SM and, as discussed in [25], the implementation can be based on a Dynamic Electrical Model (DEM) or approximated as a Quasi-Stationary Electrical Model (QSEM). Both implementations will be evaluated in this paper. The Inertia Model and the frequency control according to Fig. 1 provide the frequency and phase angle for synchronization of the inner loop current control with the ac-side grid voltage. Compared to the implementation presented in [25], the control scheme defined by Fig. 2 a) and b) is completed with circulating current controllers and balancing algorithms for the MMC, based on the implementation presented in [21].

B. *Voltage Controlled VSM*

A Voltage Controlled VSM (VCVSM) is considered based on the implementation from [21]. Most of the general control blocks for the VCVSM are identical to the CCVSM, including the inertia model, the reactive power controller, as well as the circulating current controller and modulation strategies for operating the MMC. However, the virtual impedance implementation and the inner loop control is different, as specified by Fig. 2 c). In this case, a quasi-stationary virtual impedance is configured to generate a *dq*-frame voltage reference, instead of a current reference as in the CCVSM. This voltage reference is actuated by a *dq*-frame voltage controller providing the references for the inner loop current controller, according to the VSM implementation from [26].

C. *Frequency-derivative-based inertia emulation*

An overview of the control structure for the *df/dt* IE control is shown in Fig. 3. The implementation is based on the control strategy evaluated for a 2-level VSC in [27], but adapted for operating an MMC in the same way as the VSM-based control strategies. The inner control loops, including the ac-side current controller and the circulating current controller, are again identical to the other schemes. The control system is synchronized to the grid with a PLL, assuming the same PLL implementation as used for frequency estimation in the VSM-based control strategies. The active and reactive current references are provided by PI-controllers regulating the active and reactive power flow, respectively, and the incremental power reference for the inertia emulation is generated according to (4).

This is the accepted version of an article published in Proceeding 45th Annual Conference of the IEEE Industrial Electronics Society - IECON 2019
http://dx.doi.org/10.1109/IECON.2019.8927704

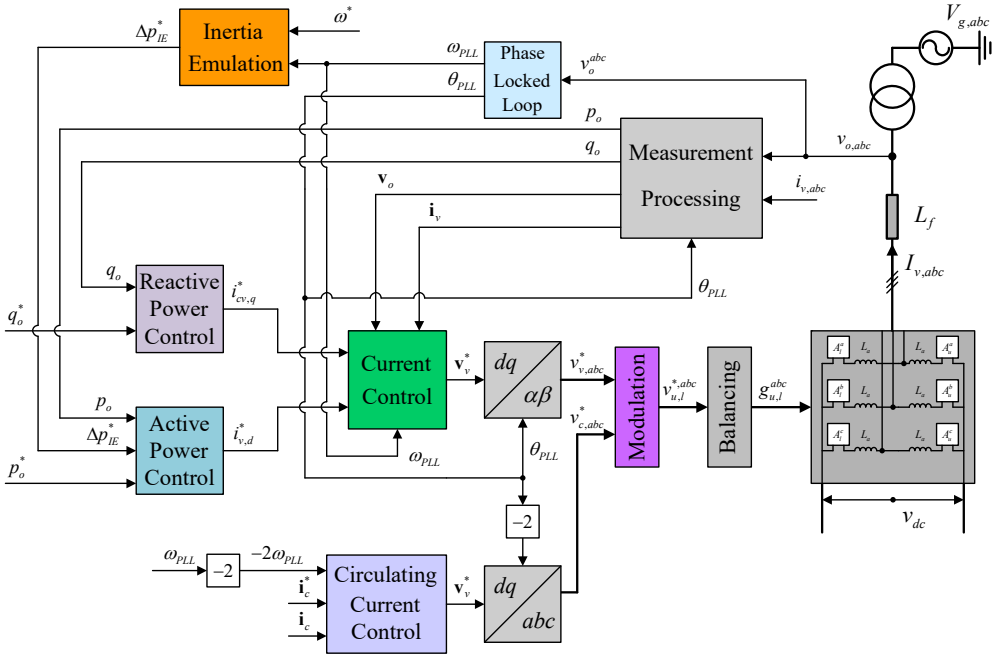

Fig. 3. Control structure for frequency derivative-based inertia emulation (df/dt IE)

TABLE I
MAIN PARAMETERS OF THE REDUCED-SCALE MMC PROTOTYPES

Converter parameters	Reference	18 HB model	6 HB model
Rated power	1059MVA	60 kVA	60 kVA
Rated DC voltage	640 kV	700V	700V
Rated AC voltage|	333 kV	400V	400V
Rated current	1836A	83A	83A
Cells per arm	401 HB	18 HB	6 HB
Nominal cell voltage	2 kV	44 V	133 V
Arm inductance	50 mH	1,4 mH	1,4 mH
Cell capacitance	10 mF	19,8 mF	7,5 mF

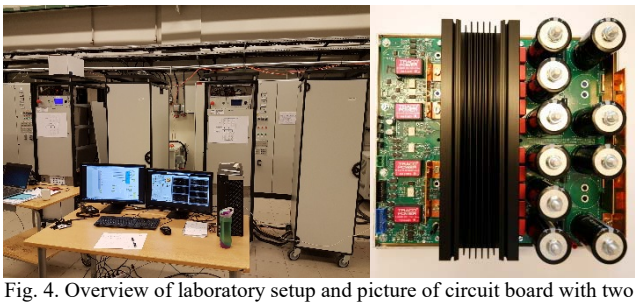

Fig. 4. Overview of laboratory setup and picture of circuit board with two half-bridge sub-modules

IV. EXPERIMENTAL SETUP FOR P-HIL TESTING

In this section, the configuration of the P-HiL platform used for testing various types of the MMC-based strategies for inertia emulation will be briefly described. This configuration allows for interfacing the physical hardware for laboratory scale emulation of an MMC-based HVDC system with a real-time simulation of a power system. The physical part of the experiment is formed by connecting two MMCs in back-to-back configuration. One MMC acts as a rectifier terminal of the HVDC transmission line and regulates the dc voltage while the other MMC is operated with Virtual Inertia Control (VIC). The ac-side of both MMCs are connected to a grid emulator with controllable voltage outputs for actuating the results from real-time simulations.

A. Modular Multilevel Converter (MMC)

The MMC prototypes used for the experiments are designed for small-scale emulation of HVDC converter terminals. The main parameters of the MMC prototypes are listed in Table I, and are resulting from a design intended for scaling the internal energy dynamics of a real HVDC converter terminal with parameters according to [28]. As shown in the table, two different MMC designs are used in the experiments: one with 18 half-bridge (HB) modules per arm and the other with 6 HB modules per arm. In the experiments, the MMC with 18 modules per arm (MMC – N18) is used for inertia emulation, while the MMC with 6 modules per arm (MMC – N6) is used for controlling the dc voltage. A picture of the laboratory setup and the circuit boards constituting the individual modules of the MMC is shown in Fig. 4.

The main control loops for operating the MMCs, e.g. voltage and current controllers, circulating current controllers, and the VIC, are implemented in MATLAB/Simulink and executed in real-time on the real-time target of an OPAL-RT platform (OP5600). However, the sorting algorithm for the internal voltage balancing and the generation of the gate signals for the individual converter modules are generated individually for each arm of the converter by a distributed control system. Further information about the implementation is provided in [21]. The communication for transferring the command signals from the OPAL-RT target to the MMCs and the measurement and monitoring signals sent back from the MMCs is executed via a dedicated high-speed, full-duplex fiber-optical bus operating at 5 Mbit/s.

This is the accepted version of an article published in Proceeding 45th Annual Conference of the IEEE Industrial Electronics Society - IECON 2019
http://dx.doi.org/10.1109/IECON.2019.8927704

B. Grid emulator

The P-HiL testing is enabled by a switch-mode grid emulator with high control bandwidth operated as a power amplifier. This grid emulator is a 200 kVA COMPISO System Unit (CSU) manufactured by EGSTON Power, with six COMPISO Digital Amplifiers (CDA) outputs. The six output channels can be controlled independently in various configurations, but in this P-HiL setup the CDAs are configured to provide two independent and controllable three-phase voltage sources. For the practical testing, one three-phase output is controlled as a constant voltage source with a fixed frequency and supplies the rectifier terminal of the scaled-down HVDC system. The other three-phase output is utilized to actuate the voltage at one bus of a small power system simulated in real-time.

The grid emulator is controlled from the same OPAL-RT platform as the MMCs via a low latency fiber optic connection. The P-HiL implementation is based on the ideal transformer model (ITM) scheme [29], where the grid emulator acts as a voltage source while the measured currents are fed back in real-time to ideal current sources in the numerical simulation.

C. Real-time simulation platform (OPAL-RT)

The OPAL-RT platform is the core part of the P-HiL experimental configuration, as it executes parts of the real-time control of the MMCs as well as the real-time simulation model controlling the grid emulator. The simulation models created in MATLAB/Simulink are automatically translated into C code that in turn is compiled for execution on the OPAL-RT platform. The procedure of compiling, loading, and executing the model on the OPAL-RT target is based on the RT-LAB dedicated software interface which also provide means for monitoring of the simulation and for online manipulation of the model parameters during simulation. The OPAL-RT used in this experiment is an OP5600 with an extension box for interfacing the grid emulator and the converters via fiber optic. The communication with the grid emulator and the MMCs relies on two separate high-speed optical buses, respectively, that can transfer data at the rate up to 5 Mbit/s.

D. Overview of experimental setup and real-time simulations

An overview of the full experimental setup for P-HiL testing is shown in Fig. 5. In this setup, the OPAL-RT platform is mainly responsible for the following two tasks:

- Real-time execution of MMC control, including VIC
- Real-time simulation of the power system actuated by the grid emulator.

The real time simulation and the controls of the MMC are executed with a 100 us time step.

As indicated in Fig. 5, the MMC-N6 is connected to Terminal 2 of the grid emulator, which is operated as a voltage source with fixed frequency and voltage amplitude as specified from the OPAL-RT platform. The OPAL-RT platform is also implementing the control system for this

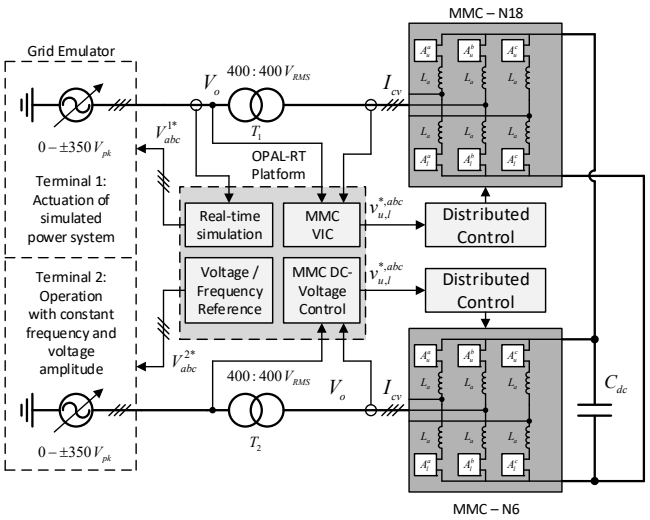

Fig. 5. System configuration for PHiL testing of MMC-based VIC

MMC, which is a conventional control strategy with a similar structure as shown in Fig. 3 but with a dc voltage controller providing the *d*-axis current reference.

The MMC-N18 is connected to Terminal 1 of the grid emulator and can be operated with any of the investigated VIC strategies. The real-time simulation implemented for operating Terminal 1 of the grid emulator is configured to operate either as a strong grid with a fixed frequency and a constant voltage, or as a small islanded power system. The simulated islanded power system configuration includes a synchronous generator with traditional governors and automatic voltage regulators (AVR), supplying its power to a bank of adjustable resistive loads via a line impedance. The load resistance can be changed online during the real-time simulation to impose perturbations in the simulated system. The actuated voltage of the simulated system is scaled to a nominal value of 150 V peak phase voltage, while the dc voltage reference for the MMC-based interconnection is 420 V during the experiments.

E. Controllers tuning

The three control schemes share an identical inner current control loop and the control of the circulating current. The current control is based on PI regulators in a dq-frame whose regulators gains have been initially set according to the Modulus Optimum tuning [26], and then adjusted to ensure satisfactory performance to reference step changes on the experimental setup. A similar approach has been applied to the voltage controller in the VCVSM but with an initial guess based on the application of the Symmetrical Optimum tuning.

The tuning of the external loops and the inertia emulation are aimed at producing comparable dynamic performance. This translated into setting equal active power droop coefficients while, for simplicity, the reactive power control has been disabled by setting a zero droop gain. Furthermore, the virtual inertia and the damping coefficients are equal for all the VSM-based schemes. The *df/dt* IE control can also be tuned with an equivalent value for the inertia. However, the damping is more linked to the time constant of the low pass filtering applied in the estimation of the frequency derivative.

This is the accepted version of an article published in Proceeding 45th Annual Conference of the IEEE Industrial Electronics Society - IECON 2019
http://dx.doi.org/10.1109/IECON.2019.8927704

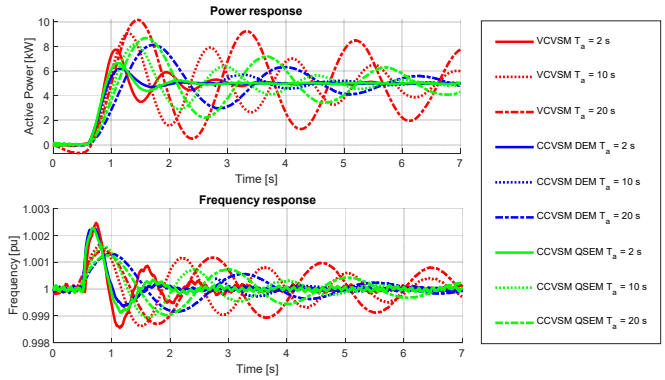

Fig. 6. Output power and virtual inertia speed in response to a step in the power reference for VSM connected to infinite inertia grid

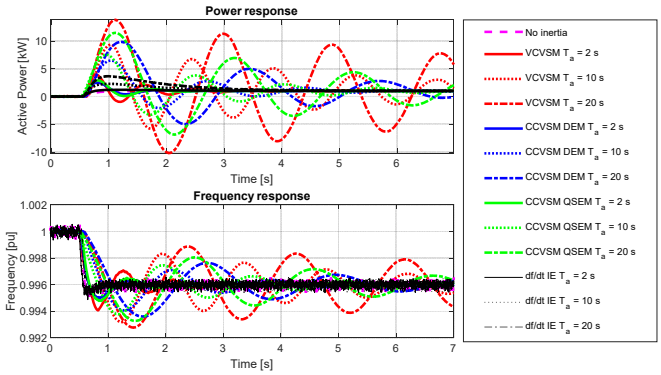

Fig. 7. Output power and virtual inertia speed in response to a step in the grid frequency for VSM connected to infinite inertia grid

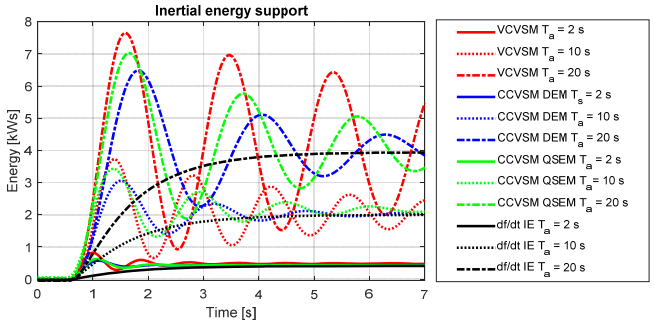

Fig. 8. Net energy support in response to a step in the grid frequency

V. Experimental Results

As mentioned, two grid scenarios have been considered for the P-HiL experiments, assuming either a strong grid with infinite inertia or an islanded grid with a low equivalent inertia. All the presented VIC strategies have been tested for different values of the inertia in order to highlight the parametric sensitivity. The aim of the experimental tests is to comparatively assess the benefits of the schemes from a power system perspective. Thus, the focus has been in displaying the capability of the schemes to support the external grid and to avoid introducing poorly damped oscillations.

A. Evaluated variables

For comparing the performances of the investigated VIC schemes, the following variables are displayed and discussed:

i) Power injected from the converter into the grid: this variable provides a relevant measure of the VIC performance since it is directly correlated with the capabilities for supporting the grid. The power flow highlights also the speed of response with respect to external disturbances and the delays in providing inertial support. Ideally the power injected should follow the dynamics of the swing equation. Thus, a main aspect to assess are the deviations introduced by the different implementations. However, the power should be always bounded within the limits of the converter ratings.

ii) Frequency measured from the converter: this variable also provides meaningful insight in the operation of the schemes and the emulated dynamics for providing the inertia support. For the VSM based schemes this frequency can be obtained as the internal speed of the virtual inertia. For the *df/dt* IE scheme the frequency can be obtained from the PLL.

iii) Inertial energy support: another relevant comparative assessment can be based on the energy that the VIC schemes can provide. The exchanged energy can in general be obtained by integrating the power. However, a more meaningful comparison can be based on the energy difference provided by the inertial support scheme with reference to an identical scheme without the inertia support. Thus, a conventional control structure according to Fig. 3, but with zero virtual inertia, is assumed as a point of reference for all experiments. Since all the evaluated schemes will reach the same operating condition in steady state, the inertial energy support provided by the different VI control strategies (VI_x) in response to a disturbance at time $t = t_0$ can be calculated as [45]:

$$\Delta E_{VI,x} = \int_{t_0}^{\infty} \left(P_o(VI_x) - P_{o,df/dt\ IE}\left(T_a = 0\right) \right) dt \qquad (6)$$

where $P_o(VI_x)$ is the power injected for any case x of VIC while $P_{o,df/dt\ IE}\ (T_a=0)$ is the power resulting from operation with a conventional control strategy without virtual inertia.

The dynamic response of each scheme will be affected by the tuning of the controllers and the parameters of the inertia representation in the swing equation. Thus, as explained in section IV.E, the schemes have been implemented with identical parameters wherever possible in order to perform a representative comparison.

B. Operation with strong grid conditions

In a first operating scenario, the converter is assumed to be connected to a grid with infinite inertia. Thus, the grid imposes both voltage and frequency and it is modelled as an ideal three phase voltage source. The response of the VSM schemes to a step of 5 kW in the power reference for the converter is displayed in Fig. 6. The power injected and the internal frequency show a similar overall behavior and tend to the same steady state conditions (unchanged frequency and an increase of the power corresponding to the step). However, the VCVSM is noticeably more oscillatory and provides a less damped response, especially with high values of inertia.

The response to a step of 0.04 Hz in the grid frequency are displayed in Fig. 7 and Fig. 8. The response indicates that higher values of inertia lead to higher peak power as expected. Moreover, consistently with the previous results, the VCVSM response provides slightly higher peak power but is visibly more oscillatory and less damped. The *df/dt* IE scheme generates comparatively less inertia support. Finally, the inertial energy support presented in Fig. 8 confirm again the same qualitative results.

This is the accepted version of an article published in Proceeding 45th Annual Conference of the IEEE Industrial Electronics Society - IECON 2019
http://dx.doi.org/10.1109/IECON.2019.8927704

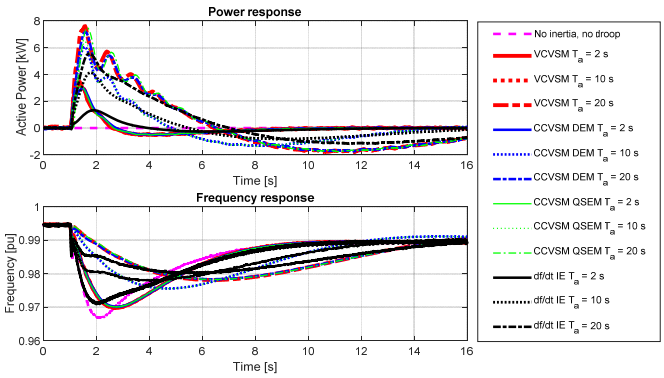

Fig. 9. Output power and measured frequency in response to a load step for inertia support schemes connected to limited inertia grid

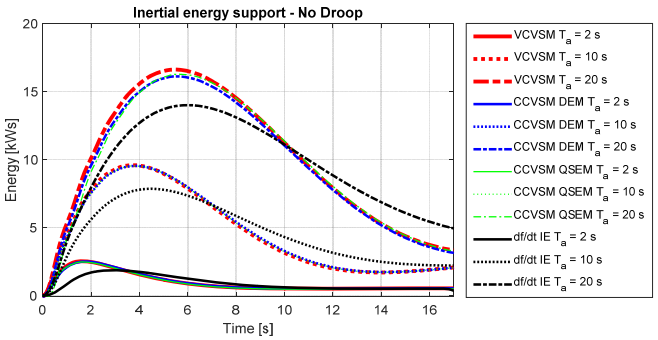

Fig. 10. Net energy support in response to a load step for inertia support schemes connected to limited inertia grid

C. *Operation with P-HiL simulation of islanded grid*

The second operating scenario is the simulated external grid with a low equivalent inertia, corresponding to either an islanded power system or smaller part of a larger grid when operated in islanded mode. A disturbance in the isolated grid is triggered by connecting an additional load. This reflects in an increase of the power drawn from the equivalent synchronous generator of the grid and a corresponding transient in the local grid frequency. Results for this scenario are presented in Fig. 9 and Fig. 10 for a case when a power-frequency droop is not included in the control of the MMC terminal. Equivalent results when the power-frequency droop is activated in all control schemes, including the reference case without VIC control, are presented in Fig. 11 and Fig. 12.

In these results, the differences between the evaluated control strategies are less pronounced than for the case of a string grid, especially between the VSM-based control schemes. The *df/dt* IE scheme in general provide a relatively smaller peak support and a more delayed response. Again, a higher value of the inertia corresponds also to a higher degree of grid support and higher value of the peak power injected in the grid. The higher support provided with more virtual inertia translates in a less deep frequency nadir. Furthermore, the case without power-frequency droop results in significantly higher inertial energy support from the MMC terminal. The main reason is that all the control system implementations for the MMC terminal are fast enough for the droop control to provide a transient power support that helps to reduce the frequency nadir of the local generator. Thus, the droop control itself is also helping to improve the frequency nadir independently of the VIC, as can be seen by comparing Fig. 9 and Fig. 11.

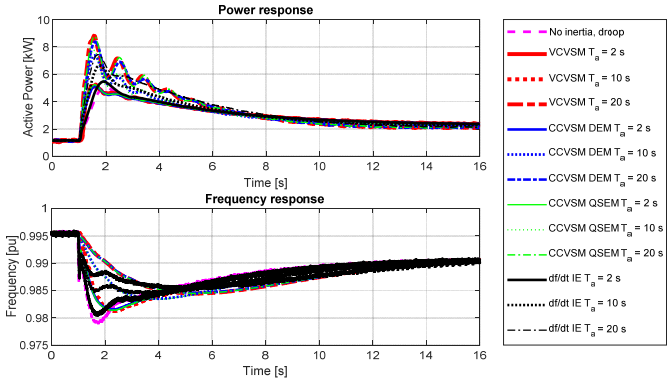

Fig. 11. Output power and measured frequency in response to a load step for inertia support schemes connected to limited inertia grid

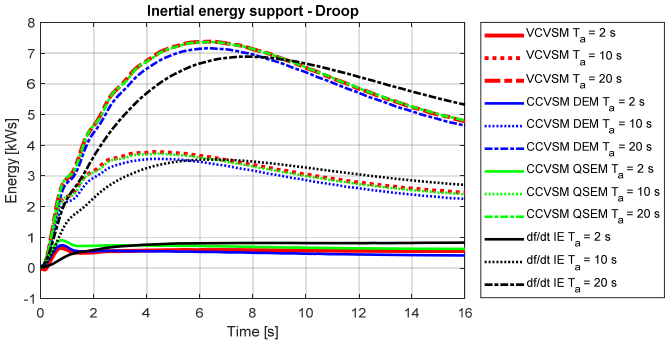

Fig. 12. Net energy support in response to a load step for inertia support schemes connected to limited inertia grid

TABLE II
INERTIAL ENERGY SUPPORT PROVIDED TO THE LOCAL GRID

Type	Droop	Inertia	Peak Energy [kWs]	Time at peak [s]
CCVSM DEM	Yes	2	0,74	0,79
	Yes	10	3,56	4,40
	Yes	20	7,16	6,34
	No	2	2,51	1,74
	No	10	9,53	3,85
	No	20	16,11	5,53
CCVSM QSEM	Yes	2	0,91	0,79
	Yes	10	3,72	4,47
	Yes	20	7,36	6,40
	No	2	2,48	1,64
	No	10	9,53	3,73
	No	20	16,27	5,59
VCVSM	Yes	2	0,65	0,79
	Yes	10	3,78	4,42
	Yes	20	7,38	6,39
	No	2	2,53	1,61
	No	10	9,59	3,79
	No	20	16,61	5,47
DF/DT	Yes	2	0,83	16,00
	Yes	10	3,53	6,48
	Yes	20	6,89	7,76
	No	2	1,86	2,93
	No	10	7,85	4,47
	No	20	14,00	6,01

A summary of the results from the evaluated cases, with the peak value of the additional energy provided by the VIC and the corresponding time when the energy peak occurs, is reported in the Table II. Such information can be utilized to evaluate if the required energy for a certain inertial response can be provided from the HVDC interconnection or not.

This is the accepted version of an article published in Proceeding 45th Annual Conference of the IEEE Industrial Electronics Society - IECON 2019
http://dx.doi.org/10.1109/IECON.2019.8927704

VI. CONCLUSION

This paper presented a comparison of four different control system implementations for providing virtual inertia support to a grid from an MMC-based HVDC system. The assessment is based on experimental tests on a laboratory-scale point-to-point configuration with two MMCs, where one converter provides inertia support to an emulated grid with a P-HiL approach. The tests aimed at providing a fair comparison and to identify the influence of the implementation on the inertial support and on the sensitivity to the inertia constant. The experimental results confirm the expected performance of inertia support to the grid by transient power injection and how a higher value of the virtual inertia corresponds to higher net energy transfer compared to a reference case without inertial support. Moreover, the results highlight that when connected to a strong grid, the dynamic responses of the considered schemes present non-negligible differences, with the VCVSM scheme being the most oscillatory. This demonstrates the importance of considering the full scheme when assessing the performance of control strategies for providing inertia support. Indeed, the implementation of the same swing equation ensure only the same behavior of the schemes for slow dynamics and at steady state. Differences are much less noticeable when operating in grids with low equivalent inertia and transients dominated by the inertial dynamics. In these conditions an analysis based on the simplified swing equation while neglecting the remaining loops will be more reasonable than for the case of a strong grid.

REFERENCES

[1] J. O'Sullivan, A. Rogers, D. Flynn, P. Smith, A. Mullane, M. O'Malley, "Studying the Maximum Instantaneous Non-Synchronous Generation in an Island System – Frequency Stability Challenges in Ireland," in *IEEE Trans. on Power Syst.*, Vol. 29, No. 6, Nov. 2014, pp. 2943-2951

[2] M. Yu, A. Dyśko, C. Booth, A. Roscoe, J. Zhu, H. Urdal, "Investigations on the Constraints relating to Penetration of Non-Synchronous Generation (NSG) in Future Power Systems," in *Proceedings of the 2015 Protection, Automation and Control (PAC) World Conference*, Glasgow, UK, 29 June – 2 July 2015, 9 pp.

[3] Y. Wang, V. Silva, M. Lopez-Botet-Zulueta, "Impact of high penetration of variable generation on frequency dynamics in the continental Europe interconnected system," in *IET Renewable Power Generation*, Vol. 10, No. 1, January 2016, pp. 10-16

[4] Statnett, Fingrid, Energinet.dk, Svenska Kraftnät, "Challenges and Opportunities for the Nordic Power System," August 2016

[5] H.-P. Beck, R. Hesse, "Virtual Synchronous Machine," in *Proceedings of the 9th International Conference on Electrical Power Quality and Utilisation*, Barcelona, Spain, 9-11 October 2007, 6 pp.

[6] K. Sakimoto, Y. Miura, T. Ise, "Stabilization of a power system with a distributed generator by a virtual synchronous generator function," in *Proceedings of the 8th International Conference on Power Electronics – ECCE Asia*, Jeju, Korea, 30 May- 3 June 2011, 8 pp.

[7] Q.-C. Zhong, G. Weiss, "Synchronverters: Inverters That Mimic Synchronous Generators," *IEEE Transactions on Industrial Electronics*, vol. 58, no. 4, April 2011, pp. 1259-1267

[8] S. D'Arco, J. A. Suul, "Virtual Synchronous Machines – Classification of Implementations and Analysis of Equivalence to Droop Controllers for Microgrids," in *Proceedings of IEEE PowerTech Grenoble 2013*, Grenoble, France, 16-20 June 2013, 7 pp.

[9] H. Bevrani, T. Ise, Y. Miura, "Virtual synchronous generators: A survey and new perspectives," in *International Journal of Electric Power and Energy Systems*, vol. 54, pp. 244–254, January 2014

[10] H. Alrajhi Alsiraji, R. El-Shatshat, "Comprehensive assessment of virtual synchronous machine based voltage source converter controllers," in *IET Generation, Transmission, Distribution*, vol. 11, no. 7, pp. 1762–1769, may 2017

[11] Booth, G. P. Adam, A. J. Roscoe, C. G. Bright, "Inertia Emulation Control Strategy for VSC-HVDC Transmission Systems," in *IEEE Trans.s on Power Systems*, Vol. 28, No. 2, May 2013, pp. 1277-1287

[12] J. Zhu, J. M. Guerrero, W. Hung, C. D. Booth, G. P. Adam, "Generic inertia emulation controller for multi-terminal voltage-source-converter high voltage direct current systems," in *IET Renewable Power Generation*, Vol. 8, No. 7, September 2014 pp. 740-748

[13] M. Guan, W. Pan, J. Zhang, Q. Hao, J. Cheng, X. Zheng, "Synchronous Generator Emulation Control Strategy for Voltage Source Converter (VSC) Stations," in *IEEE Transactions on Power Systems*, Vol. 30, No. 6, November 2015, pp. 3093-3101

[14] K. Rouzbehi, W. Zhang, J. I. Candela, A. Luna, P. Rodriguez, "Unified reference controller for flexible primary control and inertia sharing in multi-terminal voltage source converter-HVDC grids," in *IET Gen., Trans.& Distr.*, Vol. 11. No. 3, Feb. 2017, pp.750-758

[15] E. Rakhshani, P. Rodríguez, "Inertia Emulation in AC/DC Interconnected Power Systems Using Derivative Technique Considering Frequency Measurement Effects," in *IEEE Transactions on Power Systems*, Vol. 32, No. 5, September 2017, pp. 3338-3351

[16] W. Zhang, K. Rouzbehi, A. Luna, G. B. Gharehpetian, P. Rodriguez, "Multi-terminal HVDC grids with inertia mimicry capability," in *IET Renewable Power Generation*, Vol. 10, No. 6, July 2016, pp. 752-760

[17] R. Aouini, B. Marinescu, K. B. Kilani, M. Elleuch, "Synchronverter-Based Emulation and Control of HVDC Transmission," in *IEEE Trans. on Power Systems*, Vol. 31, No. 1, January 2016, pp. 278-286

[18] R. Aouini, B. Marinescu, K. B. Kilani, M. Elleuch, "Stability improvement of the interconnection of weak AC zones by synchronverter-based HVDC link," in *Electric Power System Research*, Vol. 142, January 2017, pp. 112-124

[19] B. Peng, X. Yin, J. Shen, J. Wang, "Application of Virtual Synchronization Control Strategy in MMC based VSC-HVDC System," in *Proceedings of the 2014 IEEE PES Asia-Pacific Power and Energy Engineering Conference*, APPEEC 2014, Kowloon, Hong Kong, 7-10 December 2014, 6 pp.

[20] C. Verdugo, J. I. Candela, P. Rodriguez, "Grid Support Functionalities based on Modular Multilevel Converters with Synchronous Power Control," in *Proceedings of the 2016 IEEE International Conference on Renewable Energy Research and Applications*, ICRERA 2016, Birmingham, UK, 20-23 November 2016, pp. 572-577

[21] S. D'Arco, G. Guidi, J. A. Suul, "Operation of a Modular Multilevel Converter Controlled as a Virtual Synchronous Machine," in *Proceedings of the International Power Electronics Conference*, IPEC 2018 ECCE Asia, Niigata, Japan, 20-24 May 2018, 8 pp.

[22] P. Kundur, "*Power System Stability and Control*," New York: McGraw-Hill Education, 1994

[23] D. Duckwitz, B. Fisher, "Modeling and Design of df/dt-based Inertia Control for Power Converters," in *IEEE J. Emerging and Selected Topics in Power Electron.* , Vol. 5, No. 4, pp. 1553-1564, Dec. 2017

[24] J. Ekanayake, N. Jenkins, "Comparison of the Response of Doubly Fed and Fixed-Speed Induction Generator Wind Turbines to Changes in Network Frequency," in *IEEE Transactions on Energy Conversion*, Vol. 19, No. 4, pp. 800-802, December 2004

[25] O. Mo, S. D'Arco, J. A. Suul, "Evaluation of Virtual Synchronous Machines with Dynamic or Quasi-stationary Machine Models," in *IEEE Trans. on Ind. Electron.*, Vol. 64, No. 7, pp. 5952-5962, Jul 2017

[26] S. D'Arco, J. A. Suul, O. B. Fosso, "A Virtual Synchronous Machine Implementation for Distributed Control of Power Converters in SmartGrids," in *El. Power Syst. Res.*, Vol. 122, pp. 180-197, May 2015

[27] J. A. Suul, S. D'Arco, "Comparative Analysis of Small-Signal Dynamics in Virtual Synchronous Machines and Frequency-Derivative-Based Inertia Emulation," in *Proceedings of the 18th International Conference on Power Electronics and Motion Control*, PEMC 2018, Budapest, Hungary, 26-30 August 2018, pp. 344-351

[28] J. Peralta, H. Saad, S. Dennetiére, J. Mahseredjian S. Nguefeu, "Detailed and averaged models for a 401-level MMC-HVDC system" *IEEE Trans. on Power Del.* Vol 27 No. 3 July 2012, pp.1501-1508

[29] W. Ren, M. Steurer, T. L. Baldwin, "Improve the Stability and the Accuracy of Power Hardware-in-the-Loop Simulation by Selecting Appropriate Interface Algorithms," in *IEEE Transactions on Industry Applications*, Vol. 44, No. 4, pp. 1286-1294, July/August 2008,

This is the accepted version of an article published in Proceeding 45th Annual Conference of the IEEE Industrial Electronics Society - IECON 2019
http://dx.doi.org/10.1109/IECON.2019.8927704